

# ***N*-Terminal seven-amino-acid extension simultaneously improves the pH stability, optimal temperature, thermostability and catalytic efficiency of chitosanase CsnA**

Yujuan Han · Peixin Gao · Wengong Yu · Xinzhi Lu

Received: 24 July 2017 / Accepted: 31 August 2017 / Published online: 13 September 2017  
© Springer Science+Business Media B.V. 2017

## **Abstract**

**Objective** To determine the effects of the extra *N*-terminal seven-amino-acid sequence on the function of chitosanase CsnA.

**Results** Sequence and structure analysis indicated that the mature CsnA contains a seven-amino-acid extension in a disordered form at the *N*-terminus. To determine the function of this sequence, both mature CsnA and its *N*-terminus-truncated mutant, CsnA $\Delta$ N, were expressed in *Escherichia coli* and characterized. Compared with CsnA $\Delta$ N, CsnA exhibited a 15 °C higher temperature optimum, enhanced pH stability, thermostability and catalytic efficiency. The underlying mechanisms responsible for these changes were analyzed by circular dichroism (CD) spectroscopy. CD analysis revealed that the deletion of the *N*-terminal sequence resulted in a decrease in the  $T_m$  of

4.3 °C and this sequence altered the secondary structure of the enzyme.

**Conclusions** The *N*-terminal sequence is essential for the stability and activity of chitosanase CsnA.

**Keywords** Catalytic efficiency · Chitosanase · Kinetic parameters · *N*-terminal sequence · Thermostability

## **Introduction**

Chitosanase (EC 3.2.1.132) randomly attacks the  $\beta$ -1,4-linkages of the chitosan backbone, thereby producing bioactive chitooligosaccharides (COS). Based on structure and amino acid sequence similarities, chitosanases are mainly grouped into glycoside hydrolase (GH) families 5, 8, 46, 75 and 80 (<http://www.cazy.org>). Among these families, GH46 chitosanases have been extensively studied in terms of their catalytic features, enzymatic mechanisms and protein structures (Fukamizo and Brzezinski 1997; Saito et al. 1999). Most of characterized GH46 chitosanases consist only of a single catalytic module and the structure and function of this module have been intensively investigated. The enzymes are mostly  $\alpha$ -helical proteins, dumbbell-shaped, and are composed of two globular lobes (a major lobe and a minor lobe) separated by a substrate-binding cleft (Fukamizo and Brzezinski 1997; Saito et al. 1999). Two strictly

---

**Electronic supplementary material** The online version of this article (doi:[10.1007/s10529-017-2436-9](https://doi.org/10.1007/s10529-017-2436-9)) contains supplementary material, which is available to authorized users.

---

Y. Han · P. Gao · W. Yu · X. Lu (✉)  
Key Laboratory of Glycoscience & Glycotechnology of Shandong Province; Key Laboratory of Marine Drugs, Chinese Ministry of Education; Laboratory for Marine Drugs and Bioproducts, Qingdao National Laboratory for Marine Science and Technology; Department of Glycobiology; School of Medicine and Pharmacy, Ocean University of China, 5 Yushan Road, Qingdao 266003, China  
e-mail: luxinzhi@ouc.edu.cn

conserved residues (Glu and Asp) in GH46 enzymes are essential for catalysis (Boucher et al. 1995). These function, respectively, as a general acid and a nucleophile. Compared with the sequence of the catalytic module, terminal sequences are less conserved and even in a disordered form in chitosanases. Consequently, research on the role of the *N*- or/and *C*-terminal sequences in structure and function of the enzymes remains scarce. However, recent studies have proposed that the terminal regions have significant effects on protein soluble expression, folding and function (Hu et al. 2017; Li et al. 2014; Liu et al. 2011; Lu et al. 2016).

A GH46 chitosanase CsnA was identified from *Renibacterium* sp. QD1. It had maximum activity at pH 5.6 and stability over a wide pH range (Xing et al. 2014). Based on sequence alignment and homology modeling with the *Streptomyces* sp. N174 chitosanase (PDB code: 1CHK) as the template, the mature CsnA has an extra seven-amino-acid sequence (Ser-1-Ala-7) that did not form a regular secondary structure at the *N*-terminus and its function was unknown. The objective of this study was to examine the effect of this sequence on the enzyme function: the *N*-terminal segment has a distinct impact on optimal temperature, pH stability, thermostability and catalytic activity. To the best of our knowledge, this is the first report about the effects of terminal sequence on chitosanase. This study provides more insights into the significance of terminal region and the integration of structure and function of the enzyme.

## Materials and methods

### Strains, plasmids, and chemicals

*E. coli* DH5 $\alpha$  and BL21(DE3) were used for plasmid amplification and expression, respectively. The plasmids *pEASY-T1* (TransGen, China) and *pET-22b(+)* (Invitrogen, USA) were used for gene cloning and heterologous gene expression, respectively. Chitosan ( $\geq 90\%$  deacetylated) was purchased from Qingdao MdBio, Inc. (China).

### Gene cloning and sequence analysis

Genomic DNA of *Renibacterium* sp. QD1 was used as the template for amplification of CsnA gene (*CsnA*).

Primers used for gene cloning are shown in Supplementary Table 1. Comparison of the amino acid sequence of CsnA with known sequences was conducted with the BLASTP programs at NCBI. The Swiss-model server (<http://swissmodel.expasy.org/>) was used to build the three-dimensional structure of CsnA with the chitosanase from *Streptomyces* sp. N174 (PDB code: 1CHK) as the template, which showed the highest percentage identity (67.4%) among the available amino acid sequences. A Ramachandran plot (<http://mordred.bioc.cam.ac.uk/~rapper/rampage.php>) was used for structure validation. The molecular masses of the enzymes were predicted using Compute pI/Mw tool on the ExPASy Server ([http://web.expasy.org/compute\\_pi/](http://web.expasy.org/compute_pi/)).

### Mutant construction, protein expression and purification

Sequence and structure analysis indicated that CsnA had an extra seven-amino-acid sequence that present in the form of random coil at the *N*-terminus. To verify the function of this fragment, we cloned the mature CsnA gene without the signal peptide-coding sequence and its truncated version (CsnA $\Delta$ N) gene without the *N*-terminal sequence by PCR, respectively, with primers CsnA-F/CsnA-R and CsnA $\Delta$ N-F/CsnA $\Delta$ N-R (Supplementary Table 1). PCR products were digested by *MscI* and *HindIII* and ligated into the *pET-22b(+)* vector. The resulting plasmids, *pET-CsnA* and *pET-CsnA $\Delta$ N*, were transformed into *E. coli* BL21(DE3). The positive transformants harboring *pET-CsnA* and *pET-CsnA $\Delta$ N* were used for enzyme expression with IPTG induction (0.5 mM) at 25 °C for 60 h. The supernatants were harvested by centrifugation at 4 °C (10,000 $\times g$ , 20 min) and then applied onto a Ni-Sepharose column equilibrated with 20 mM Tris/HCl buffer (pH 8) containing 0.5 M NaCl. Protein fractions were collected and analyzed by SDS-PAGE. The protein concentration was determined using a protein assay kit.

### Enzymatic activity assay and characterization

The enzymatic activity was determined using the dinitrosalicylic acid (DNS) method. One unit (U) was defined as the amount of enzyme that released reducing sugar equal to 1  $\mu$ M glucosamine.HCl per min under standard conditions.

The pH optima and pH stability of the enzymes were measured from pH 3.6 to 10.6. The optimal temperature and thermostability were determined at 0–70 °C at the pH optimum. The  $T_{50}$  value, the temperature at which 50% of enzyme activity was retained, was calculated as described previously (Wulf et al. 2012).

#### Determination of kinetic parameters

The kinetic parameters were determined with chitosan from 1 to 10 mg/ml at 55 °C (CsnA) or 40 °C (CsnA $\Delta$ N) for 1 min.  $K_m$  and  $V_{max}$  values were calculated based on Lineweaver–Burk plots using GraphPad Prism (version 5) software (GraphPad Software Inc., La Jolla, CA). The equation  $k_{cat} = V_{max}/[E]$  was used to calculate the  $k_{cat}$  value, where  $[E]$  was the molar concentration of the enzymes used in this experiment. The experiments were carried out three times.

#### Analysis of reaction pattern and hydrolysis products

The hydrolysis products of CsnA and CsnA $\Delta$ N were determined by TLC using silica gel plates 60F 254 (Merck). Time course analysis of enzymatic hydrolysates was conducted to determine the action pattern of the enzymes according to the method described previously (Xing et al. 2014).

#### Effects of metal ions and chemical reagents on enzyme activity

The effects of metal ions and chemical reagents on enzyme activity were determined by mixing the enzyme with 1 mM  $Mn^{2+}$ ,  $Al^{3+}$ ,  $Zn^{2+}$ ,  $Ba^{2+}$ ,  $Ni^{2+}$ ,  $Fe^{3+}$ ,  $Mg^{2+}$ ,  $Ca^{2+}$ ,  $Li^+$ , SDS or EDTA under the standard conditions. The relative activity was calculated with respect to the control sample where the reaction was conducted without any additives.

#### Circular dichroism (CD) analysis

To investigate the structural difference between CsnA and CsnA $\Delta$ N, the proteins were monitored by a Jasco J-810 spectropolarimeter. The enzymes (0.1 mg/ml) in 10 mM phosphate buffer (pH 7) were subjected to

signal measurement in a 1 mm cell. All measurements were conducted three times.

Thermal denaturation curves of the proteins were obtained by monitoring the change in ellipticity  $[\theta]$  at 222 nm as the temperature increased on a Jasco J-810 spectropolarimeter. The temperature of the midpoint of transition ( $T_m$ ) was calculated by curve-fitting the resultant CD values versus temperature data on the basis of a least square analysis according to the method described previously (Liu et al. 2011).

## Results

### Sequence and structure analysis of CsnA, and protein expression

Analysis of the sequence of CsnA indicated that mature CsnA contained an extra *N*-terminal oligopeptide (7 residues), a catalytic motif of GH46 (215 residues) and an extra *C*-terminal oligopeptide (16 residues) (Fig. 1a). Three-dimensional structure of CsnA was built with *Streptomyces* sp. N174 chitosanase as the template. The Ramachandran plot showed that 96.5% of residues were in the favoured regions and 3.5% were in the allowed regions (Supplementary Fig. 1). These results indicated that side chain environments in the model of CsnA were acceptable. As shown in Fig. 1b, the 16-amino-acid extension at the *C*-terminus formed  $\beta$ -strands. However, the structural conformation of the first four amino acid residues (Ser-1-Asp-4) at the *N*-terminus was missing because the chitosanase template did not have the corresponding sequence and the retained three *N*-terminal amino acids (Leu-5-Ala-7) were present in the form of random coil. Many studies have reported that the regular secondary structures make stabilizing contributions to proteins (Sharma et al. 2008; Zhukovsky et al. 1994), thus we speculated that the *C*-terminal extension might be essential for enzyme function. Unlike the regular secondary structures, the biological significance of irregular segments still remains elusive. Therefore, in order to reveal the function of the *N*-terminal random coil, we constructed the truncated mutant CsnA $\Delta$ N (Fig. 1a). The theoretical molecular masses of CsnA and CsnA $\Delta$ N were 28.2 and 27.6 kDa, respectively.

The enzymes were expressed in *E. coli* BL21(DE3) and purified to homogeneity. The molecular weights

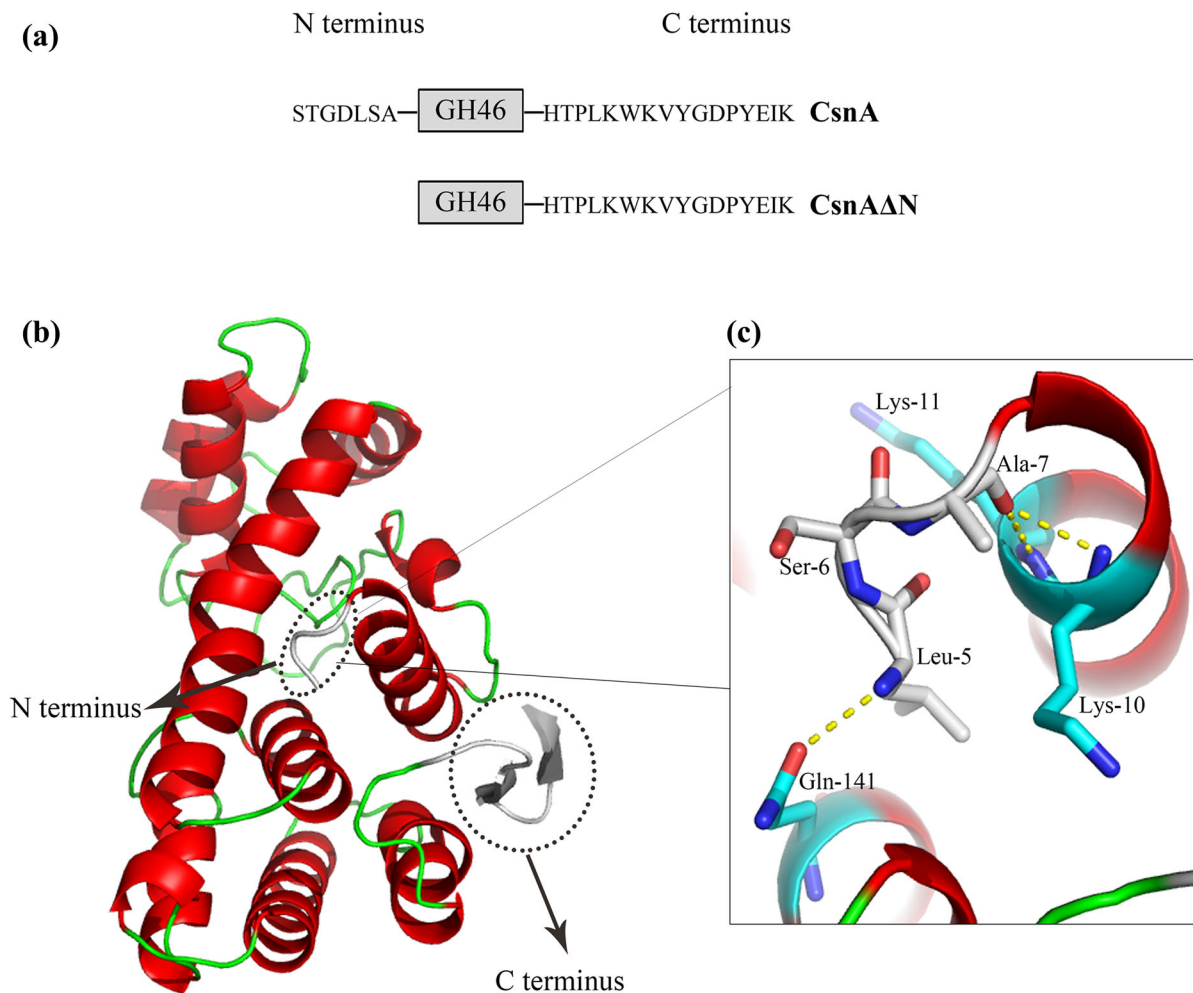


**Fig. 1** Schematic structures and three-dimensional structure. **a** Schematic structures of CsnA and its truncated mutant CsnAΔN; **b** Three-dimensional structure of CsnA. The  $\alpha$ -helix is shown as a spiral ribbon in red, the irregular coil and  $\beta$ -turn are in green. The *N*-terminus and *C*-terminus are in gray and outlined with black ovals; **c** Illustration of the polar contacts

connecting the *N*-terminus and the catalytic module. The *N*-terminal residues (Leu-5, Ser-6 and Ala-7) are shown as sticks and colored in gray. The residues involved in the polar contacts in the catalytic module are shown as sticks and colored in cyan. The polar contacts are represented by the yellow dotted lines

of CsnA and CsnAΔN estimated by SDS-PAGE were consistent with their theoretical molecular sizes (Fig. 2).

#### Enzyme properties of CsnA and CsnAΔN

Purified recombinant CsnA and its truncated derivative, CsnAΔN, had similar pH optima at 5.6 (Fig. 3a). However, CsnA was more stable over a broad pH range of 3.6 to 10.6 than CsnAΔN (Fig. 3b). Notably, CsnA retained 78–95% of its initial activity after incubation at pH 4.2–10, whereas no more than 45% of

CsnAΔN activity was retained after incubation at pH below 5 and above 8.6. These results indicated that CsnA was more stable than CsnAΔN over a broad pH range.

The optimal temperature of CsnA was 55, 15 °C higher than that of CsnAΔN (Fig. 3c). Moreover, compared with CsnAΔN, CsnA was more stable over a temperature range of 10–70 °C (Fig. 3d). CsnA retained about 80% of activity after it was incubated at 40 °C for 1 h, whereas only 20% of CsnAΔN activity was remained under the same conditions. The  $T_{50}$  of CsnAΔN decreased by 18.7 °C, compared to

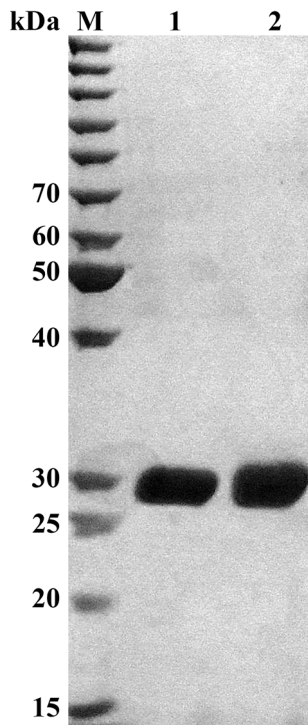


**Fig. 2** SDS-PAGE analysis of CsnA and truncated mutant CsnA $\Delta$ N. Lanes M, protein markers; Lane 1, CsnA $\Delta$ N; Lane 2, CsnA

WT. These results demonstrated that CsnA exhibited better thermostability than CsnA $\Delta$ N.

#### Kinetic parameters

As shown in Table 1, the  $K_m$  of CsnA $\Delta$ N was comparable to that of CsnA, suggesting that the *N*-terminal deletion had little effect on the substrate affinity of the enzyme. However, CsnA had higher values of  $V_{max}$ ,  $k_{cat}$ , catalytic efficiency ( $k_{cat}/K_m$ ) and specific activity than CsnA $\Delta$ N. These results indicated that the deletion of the first 7 *N*-terminal amino acids decreased the catalytic efficiency and specific activity of the enzyme.

#### Analysis of reaction pattern and hydrolysis products of CsnA and CsnA $\Delta$ N

Both CsnA and CsnA $\Delta$ N could only hydrolyze colloidal chitosan, and no activity was detected when chitosan powder was used as the substrate (data not shown). The predominant end products analyzed by

TLC were chito-biose and -triose for both CsnA and CsnA $\Delta$ N (Supplementary Fig. 2). Time course analysis of enzymatic hydrolysates indicated that both the enzymes acted in an endolytic manner (Supplementary Fig. 2). These results implied that the *N*-terminal deletion did not alter the degradation pattern of CsnA.

#### Effects of metal ions and chemical reagents on the activities of CsnA and CsnA $\Delta$ N

The effects of metal ions and chemicals on the enzyme activity were not significantly affected by the *N*-terminal deletion (Supplementary Table 2).

#### CD analysis

The  $T_m$  of CsnA $\Delta$ N was 36.06, 4.3 °C lower than that of CsnA (40.36 °C) (Fig. 4a). These results suggested that the *N*-terminal deletion certainly impaired the structural stability of the enzyme.

CD spectroscopy was used to detect possible changes in the secondary structure of truncated mutant compared to the wild-type enzyme. As shown in Fig. 4b, the CD spectra of CsnA $\Delta$ N were hardly altered by removal of the extra *N*-terminal oligopeptide. However, a detailed analysis of the CD spectra showed that the secondary structure content of CsnA $\Delta$ N was different from that of CsnA (Supplementary Table 3). Thus, we assumed that this extra *N*-terminal oligopeptide had effects on the secondary structure of CsnA.

## Discussion

Many studies have shown that terminal regions influence enzymes in different ways (Kim et al. 2011; Song et al. 2015). However, there has been no report on the relationship between terminal regions and chitosanase function. In this study, we identified an extra 7-residue *N*-terminal sequence that did not form regular secondary structure in chitosanase CsnA from *Renibacterium* sp. QD1. To explore the effect of this sequence on enzyme function and structure, we cloned the full-length CsnA gene and truncated CsnA $\Delta$ N gene, expressed them in *E. coli*, and characterized their enzymatic properties.

The deletion of the *N*-terminal amino acids led to a significant decrease in optimum temperature, pH



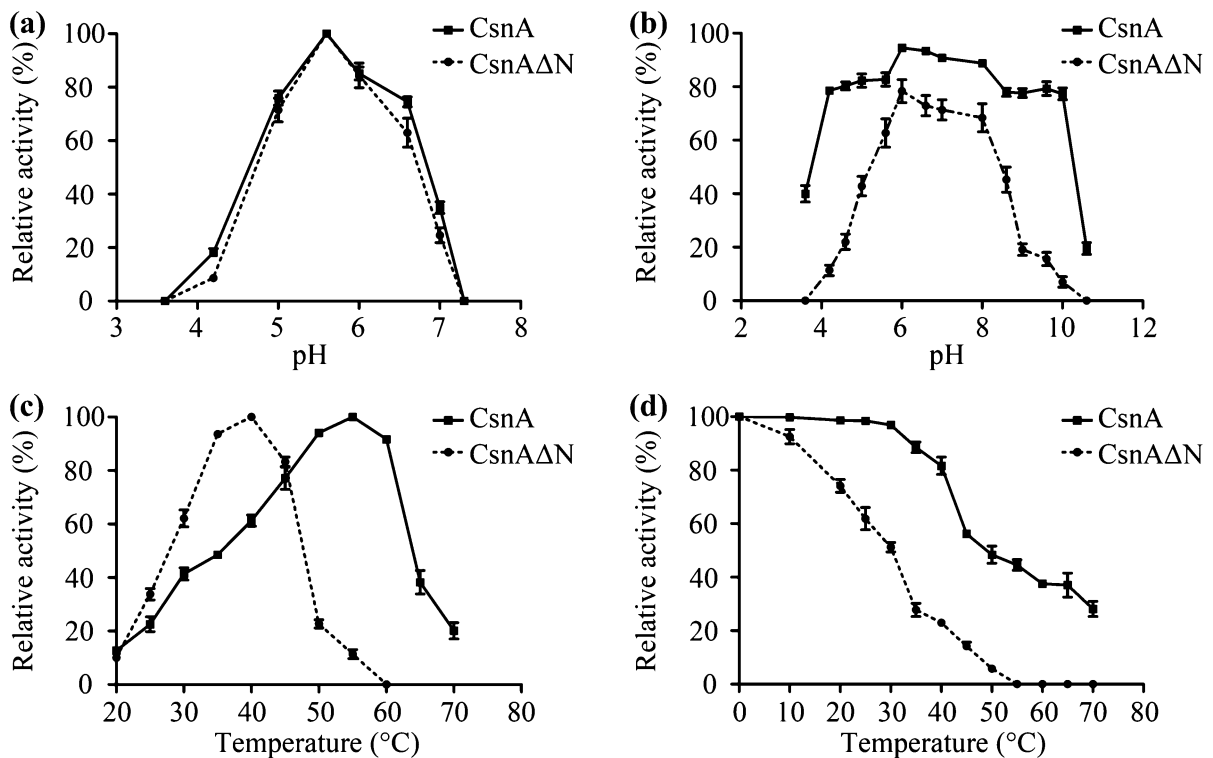


**Fig. 3** Effects of pH and temperature on enzyme activity and stability. **a** The pH optima. The pH activity profiles were estimated over the pH range of 3.6–10.6; **b** pH stability. The enzymes were preincubated in the buffers at a pH range of 3.6–10.6 at 4 °C for 12 h, and residual activities were measured under conditions described above; **c** The optimal temperatures.

The assays were conducted at 0–70 °C; **d** Thermostability. The thermostability of the enzymes was determined by measuring the residual activities after the enzymes were incubated at 0–70 °C for 1 h and then cooled at 4 °C for 10 min. Values shown are means of triplicate determinations  $\pm$  standard error (SE)

**Table 1** Kinetic parameters and specific activities of CsnA and CsnAΔN

Enzyme	$K_m$ (g/l)	$V_{max}$ ( $\mu\text{M/s}$ )	$k_{cat}$ ( $\text{s}^{-1}$ )	$k_{cat}/K_m$ (l/g.s)	Specific activity (U/mg) <sup>a</sup>
CsnA	$69 \pm 8.0$	$0.27 \pm 0.08$	$7.2 \times 10^4 \pm 85$	$1 \times 10^3$	$3.4 \times 10^2 \pm 15$
CsnAΔN	$65 \pm 7.6$	$0.25 \pm 0.09$	$5.6 \times 10^4 \pm 1.2 \times 10^2$	$8.6 \times 10^2$	$2.6 \times 10^2 \pm 19$

<sup>a</sup>Values are means  $\pm$  SD

stability and thermal stability relative to CsnA. We speculated that this terminal sequence may help to keep enzyme structure stable. Indeed, the *N*-terminal Leu-5 and Ala-7 formed three polar contacts with the Gln-141, Lys-10 and Lys-11 in the catalytic module (Fig. 1c). The importance of polar contacts in protein structural stability has been reported (Bhardwaj et al. 2010), therefore, the polar contacts around *N*-terminus might contribute to the stability of CsnA. Furthermore, the effect of this extra sequence on the structural stability of the enzyme was confirmed by the decrease

of the  $T_m$  at the time of deletion of this sequence. In addition, CD analysis revealed differences between CsnA and its truncated mutant, indicating that the *N*-terminal segment did affect the secondary structures of CsnA. It can be concluded from the above mentioned observations that the deletion of the extra *N*-terminal segment not only broke the polar contacts around *N*-terminus but also changed the secondary structure of the enzyme and thus made the local structure less compact and rigid. These results suggested that the *N*-terminal sequence confer the structural stability of

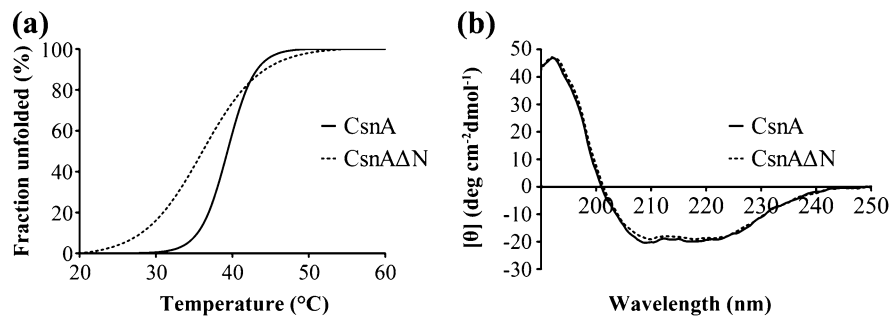


**Fig. 4** CD measurements. **a** The thermal unfolding curves of CsnA and CsnA $\Delta$ N. The denaturation CD data were measured at 222 nm from 20 to 60 °C upon heating at a rate of 2 °C/min.

CsnA, and hence, prevent the overall thermal unfolding of the enzyme at higher temperature and broader pH range.

The first seven amino acids are seated upstream of a helix and probably act as a major element for its folding. Therefore, the *N*-terminal deletion might disturb this folding. The decreased catalytic efficiency of the truncated mutant can probably be ascribed to the disturbed folding and unstable structure of the enzyme.

In summary, we identified an extra *N*-terminal sequence in disordered form in chitosanase CsnA. This oligopeptide simultaneously increased the optimal temperature, pH stability, thermostability and catalytic efficiency. Analysis of the mechanisms underlying these changes revealed that this *N*-terminal segment significantly contributed to the structural stability of the enzyme. The observations made here provide information about the biological significance of terminal regions in enzyme structure and function. In future studies, we plan to obtain the crystal structure of CsnA to get a better mechanistic understanding and then to manufacture the enzyme for better performance by engineering its *N*-terminus.

**Acknowledgements** This work was supported by the National Natural Science Foundation of China (41376144, U1406402) and Key Technologies Research and Development Program of China (2013BAB01B02).

**Supporting information** Supplementary Table 1—Primers used for gene cloning.

Supplementary Table 2—Effects of metal ions and chemical reagents on the activities of CsnA and CsnA $\Delta$ N.

Supplementary Table 3—The secondary structure contents of CsnA and CsnA $\Delta$ N.

Supplementary Fig. 1—Ramachandran plot of CsnA.

Supplementary Fig. 2—Time course analysis of enzymatic hydrolysates of CsnA (**a**) and CsnA $\Delta$ N (**b**).

**b** The CD spectra for CsnA and CsnA $\Delta$ N were recorded between 190 and 250 nm with a band width of 1 nm and a scanning speed of 100 nm/min at 25 °C

## References

- Bhardwaj A, Leelavathi S, Mazumdar-Leighton S, Ghosh A, Ramakumar S, Reddy VS (2010) The critical role of N- and C-terminal contact in protein stability and folding of a family 10 xylanase under extreme conditions. *PLoS ONE* 5:e11347
- Boucher I, Fukamizo T, Honda Y, Willick GE, Neugebauer WA, Brzezinski R (1995) Site-directed mutagenesis of evolutionary conserved carboxylic amino acids in the chitosanase from *Streptomyces* sp. N174 reveals two residues essential for catalysis. *J Biol Chem* 270:31077–31082
- Fukamizo T, Brzezinski R (1997) Chitosanase from *Streptomyces* sp. strain N174: a comparative review of its structure and function. *Biochem Cell Biol* 75:687–696
- Hu H, Chen K, Li L, Long L, Ding S (2017) Characterization of the wild-type and truncated forms of a neutral GH10 xylanase from *Coprinus cinereus*: roles of C-terminal basic amino acid-rich extension in its SDS resistance, thermostability, and activity. *J Microbiol Biotechnol* 27:775–784
- Kim YM et al (2011) Truncation of N- and C-terminal regions of *Streptococcus mutans* dextranase enhances catalytic activity. *Appl Microbiol Biotechnol* 91:329–339
- Li Z et al (2014) A C-terminal proline-rich sequence simultaneously broadens the optimal temperature and pH ranges and improves the catalytic efficiency of glycosyl hydrolase family 10 ruminal xylanases. *Appl Environ Microbiol* 80:3426–3432
- Liu L, Zhang G, Zhang Z, Wang S, Chen H (2011) Terminal amino acids disturb xylanase thermostability and activity. *J Biol Chem* 286:44710–44715
- Lu X, Wang G, Feng Y, Liu S, Zhou X, Du G, Chen J (2016) The N-terminal alpha-helix domain of *Pseudomonas aeruginosa* lipoxigenase is required for its soluble expression in *Escherichia coli* but not for catalysis. *J Microbiol Biotechnol* 26:1701–1707
- Saito J, Kita A, Higuchi Y, Nagata Y, Ando A, Miki K (1999) Crystal structure of chitosanase from *Bacillus circulans* MH-K1 at 1.6-Å resolution and its substrate recognition mechanism. *J Biol Chem* 274:30818–30825
- Sharma D, Feng G, Khor D, Genchev GZ, Lu H, Li H (2008) Stabilization provided by neighboring strands is critical for

- the mechanical stability of proteins. *Biophys J* 95:3935–3942
- Song L, Tsang A, Sylvestre M (2015) Engineering a thermostable fungal GH10 xylanase, importance of N-terminal amino acids. *Biotechnol Bioeng* 112:1081–1091
- Wulf H, Mallin H, Bornscheuer UT (2012) Protein engineering of a thermostable polyol dehydrogenase. *Enzym Microb Technol* 51:217–224
- Xing P, Liu D, Yu W-G, Lu X (2014) Molecular characterization of an endo-type chitosanase from the fish pathogen *Renibacterium* sp. QD1. *J Mar Biol Ass UK* 94:681–686
- Zhukovsky EA, Mulkerrin MG, Presta LG (1994) Contribution to global protein stabilization of the N-capping box in human growth hormone. *Biochemistry* 33:9856–9864